ARMY RESEARCH LABORATORY

Near-Resonant Two-Photon Excitation of CN

by John A. Guthrie, William R. Anderson,
Anthony J. Kotlar, Yuhui Huang,
and Joshua B. Halpern

ARL-TR-1382 June 1997

The findings in this report are not to be construed as an official Department of the Army position unless so designated by other authorized documents.

Citation of manufacturer's or trade names does not constitute an official endorsement or approval of the use thereof.

Destroy this report when it is no longer need. Do not return it to the originator.

Army Research Laboratory
Aberdeen Proving Ground, MD 21005-5066

ARL-TR-1382 **June 1997**

Near-Resonant Two-Photon Excitation of CN

John A . Guthrie, William R. Anderson, Anthony J. Kotlar
Weapons and Materials Research Directorate, ARL

Yuhui Huang, Joshua B. Halpern
Howard University

Abstract

Development of sensitive detection methods for CN is important because of applications to propellant flames. This radical plays a critical role in propellant combustion chemistry.

We have observed a strong two-photon absorption in the $B^2\Sigma^+ \leftarrow X^2\Sigma^+$ (3,0) band of CN by means of a resonant enhancement through the $A^2\Pi_i$, $v'=4$ level. Many lines are seen in the two-photon spectrum due to multiple single-photon near resonances in the $A^2\Pi_i \leftarrow X^2\Sigma^+$ (4,0) band. The detuning of the laser from these resonances varies from less than one to hundreds of wavenumbers, producing unusually large peak-intensity variations in the two-photon spectrum. This effect is not observed in two-photon transitions far from resonance. Resonant enhancement is observed over a range from $N = 5$ to 20. We know of no other molecular two-photon transition in which a near resonance produces such dramatically varying intensities over a short range of rotational levels. A calculation of the line strengths for these transitions reproduces the major features of the spectrum.

ACKNOWLEDGMENTS

J. A. Guthrie acknowledges support from the U.S. Army Research Laboratory (ARL) under the National Academy of Sciences/National Research Council (NAS/NRC) Postdoctoral Associateship Program. J. B. Halpern and Y. Huang were supported by NASA Grant 2940.

INTENTIONALLY LEFT BLANK.

TABLE OF CONTENTS

INTENTIONALLY LEFT BLANK.

LIST OF FIGURES

INTENTIONALLY LEFT BLANK.

1. INTRODUCTION

The observation of near-resonant *n*-photon electronic absorptions is rare, especially for diatomic molecules and low *n*, because few molecules possess an intermediate electronic state coupled to the ground and a higher lying excited state by strong dipole transitions. Notable exceptions include the alkali metal dimers and a few diatomic radicals. These species are characterized by low-lying electronic states, and near-resonant excitations may be allowed. The observation of single, near-resonant transitions in Na_2 and CH have been previously published [1–5]. Here, we report the observation of near-resonant two-photon absorptions in CN. These two-photon absorptions in the $B^2\Sigma^+ - X^2\Sigma^+$ (3,0) band, enhanced by single-photon near resonances in the $A^2\Pi_i$, $v'=4$ level, are exceptional because many such lines are resonantly enhanced. The detuning of the laser from the single-photon resonances varies from less than one to hundreds of wavenumbers, and the line intensities vary over a large range. Thus, this system should provide a good test of theoretical line-strength calculations.

The observation of the $B^2\Sigma^+ - X^2\Sigma^+$ (3,0) transition was unexpected because its Franck-Condon factor is small ($\approx 2 \times 10^{-5}$) [6]. Indeed, the spectrum was discovered only accidentally during a study of optical-optical double resonances involving the same three vibronic states in an atmospheric pressure flame [7]. In order to simply analysis, the two-photon spectrum reported here was recorded at room temperature and low pressure so that the collisionally enhanced optical-optical double resonances were essentially suppressed. The CN ground-state radicals were produced by the 193-nm photolysis of C_2N_2.

Two-photon line strengths have been previously calculated for a nonresonant intermediate transition in a diatomic molecule where the initial and final states conform to Hund's case (a) coupling [8–11] and for near-resonant two-photon transitions in which all states conform to either case (a) or case (b) [12]. Line strengths have also been computed in the nonresonant case for molecules in which the initial and final states conform to case (a), (b), or the intermediate case (a)–(b) coupling [13]. However, a calculation is not available wherein a near-resonant state

displays an intermediate (a)–(b) character, as does CN $A^2\Pi_i$. An appropriate calculation is given in section 3, and its results are compared to the observed spectrum in section 4.

2. EXPERIMENTAL

CN was formed by the 193-nm photolysis of C_2N_2. This process produces CN only in the $X^2\Sigma^+$ ground electronic state with about 20% of the population in the v″=1 vibrational level and the rest in the v″=0 level [14]. Rotational excitation is modest and completely relaxed to room temperature after a delay of about 150 μs at a pressure of about 200 mtorr C_2N_2. Rotational relaxation was verified by scanning the $A^2\Pi_i$ ← $X^2\Sigma^+$ (4,0) laser-induced florescence (LIF) spectrum.

A Nd:YAG-pumped dye laser, operating with DCM, was used to excite the two-photon $B^2\Sigma^+$ ← $X^2\Sigma^+$ (3,0) band. The laser was focused into the center of the experimental cell with a 350-mm focal-length lens. The Nd:YAG laser was a Spectra Physics DCR-11, and the dye laser was a PDL-II. The last amplifier was longitudinally pumped, so that the dye-laser beam had a hole in the middle, characteristic of the unstable optics in the Nd:YAG cavity. The temporal pulse width of the laser was 8 ns. Under similar conditions, with an unfocused beam, the $A^2\Pi_i$ ← $X^2\Sigma^+$ (4,0) transitions were saturated when the pulse energy was greater than 1 mJ.

The two-photon transition was observed by monitoring emission from the $B^2\Sigma^+$ → $X^2\Sigma^+$ (3,3) band through a 388-nm filter. The emitted light was detected by an eleven-stage bialkali EMI photomultiplier and averaged in a boxcar analyzer. Signals were recorded in a computerized data acquisition system that also controlled the experimental timing. Two-photon spectra were recorded at pulse energies of about 3 mJ. Higher energies saturated lines in the spectrum, as revealed by increasing line widths and growth of the weaker lines relative to the stronger ones.

3. LINE-STRENGTH CALCULATION

The line strength for a two-photon transition from ground state |g> to final state |f> is given by perturbation theory as

$$S_{gf} = \sum_{M_g M_f} \left| \sum_i \frac{\langle f|\bar{\mu}\cdot\hat{\varepsilon}|i\rangle\langle i|\bar{\mu}\cdot\hat{\varepsilon}|g\rangle}{\omega_{ig} - \omega_{fg}/2 - i\Gamma_i/2} \right|^2 \tag{1}$$

In this expression, |i> is the wave function of an intermediate state, $\bar{\mu}$ is the dipole moment of the molecule, $\hat{\varepsilon}$ is a unit vector specifying the polarization of the incident laser beam, ω_{ig} (ω_{fg}) is the transition frequency between states |i> and |g> (|f> and |g>), and Γ_i is the homogeneous width of state |i> [15]. Sums are taken first over all intermediate states |i> and then over all magnetic sublevels (M_g and M_f) in the ground and final states.

We invoke the Born-Oppenheimer approximation and use Hund's case (a) wavefunctions as a basis set, which have the form $|\Phi L\Lambda\rangle|S\Sigma\rangle|\chi\rangle|J\Omega M\rangle$, where the parameters all have their common spectroscopic meanings; $|\Phi L\Lambda\rangle$ and $|\chi\rangle$ are the electronic and vibrational parts of the wave function, respectively. The rotational part of the wavefunction in the case (a) basis is

$$\begin{aligned} |J\Omega M\rangle &= \left(\frac{2J+1}{8\pi^2}\right)^{1/2} D^{J\,*}_{M,\Omega}(\varphi\theta\chi) \\ &= (-1)^{M-\Omega}\left(\frac{2J+1}{8\pi^2}\right)^{1/2} D^{J\,*}_{-M,-\Omega}(\varphi\theta\chi) \end{aligned} \tag{2}$$

where $D^J_{M,\Omega}$ is a Wigner rotation matrix element [9–13, 15–19]. The symmetrized wavefunctions for the $^2\Sigma^+$ states are [16, 18]

$$\left|{}^2\Sigma^{+\,e/f}\right\rangle = \frac{|\Phi 00\rangle}{\sqrt{2}}|\chi\rangle\left\{\left|\tfrac{1}{2}\tfrac{1}{2}\right\rangle\left|J\,\tfrac{1}{2}M\right\rangle \pm \left|\tfrac{1}{2}-\tfrac{1}{2}\right\rangle\left|J-\tfrac{1}{2}M\right\rangle\right\} \tag{3}$$

and for the $^2\Pi$ substates they are

$$\left|{}^2\Pi_{1/2}{}^{e/f}\right\rangle = \frac{|\chi\rangle}{\sqrt{2}}\left\{|\Phi 11\rangle\left|\tfrac{1}{2}-\tfrac{1}{2}\right\rangle\left|J\,\tfrac{1}{2}M\right\rangle \pm |\Phi 1-1\rangle\left|\tfrac{1}{2}\tfrac{1}{2}\right\rangle\left|J-\tfrac{1}{2}M\right\rangle\right\}$$

and

$$\left|{}^2\Pi_{3/2}{}^{e/f}\right\rangle = \frac{|\chi\rangle}{\sqrt{2}}\left\{|\Phi 11\rangle\left|\tfrac{1}{2}\tfrac{1}{2}\right\rangle\left|J\,\tfrac{3}{2}M\right\rangle \pm |\Phi 1-1\rangle\left|\tfrac{1}{2}-\tfrac{1}{2}\right\rangle\left|J-\tfrac{3}{2}M\right\rangle\right\} \tag{4}$$

In these expressions the upper (lower) sign is chosen for e- (f-) parity levels. The $^2\Sigma^+$ $F_1(F_2)$ levels have e- (f-) parity. In order to describe the Hund's case (a)-(b) intermediate coupling for the $^2\Pi_i$ state we define

$$\left|F_1{}^{e/f}\right\rangle = \alpha\left(\tfrac{1}{2}, J-\tfrac{1}{2}\right)\left|{}^2\Pi_{1/2}{}^{e/f}\right\rangle + \alpha\left(\tfrac{3}{2}, J-\tfrac{1}{2}\right)\left|{}^2\Pi_{3/2}{}^{e/f}\right\rangle$$

and

$$\left|F_2{}^{e/f}\right\rangle = \alpha\left(\tfrac{1}{2}, J+\tfrac{1}{2}\right)\left|{}^2\Pi_{1/2}{}^{e/f}\right\rangle + \alpha\left(\tfrac{3}{2}, J+\tfrac{1}{2}\right)\left|{}^2\Pi_{3/2}{}^{e/f}\right\rangle \tag{5}$$

where J -1/2 = N for the F_1 levels and J +1/2 = N for the F_2 levels [13, 16–19]. In these expressions the coefficients α are defined as [19]

$$\alpha\left(\tfrac{1}{2}, J-\tfrac{1}{2}\right) = \alpha\left(\tfrac{3}{2}, J+\tfrac{1}{2}\right) = \left(\frac{1+ZU}{2}\right)^{1/2}$$
$$-\alpha\left(\tfrac{1}{2}, J+\tfrac{1}{2}\right) = \alpha\left(\tfrac{3}{2}, J-\tfrac{1}{2}\right) = \left(\frac{1-ZU}{2}\right)^{1/2} \tag{6}$$

and
$$U = \left[4\left(1-\frac{2D_v}{B_v}X-\frac{\gamma_v}{2B_v}\right)^2\left(J+\tfrac{1}{2}\right)^2 + \left(Y-\frac{\gamma_v}{B_v}\right)\left(Y-4+\frac{8D_v}{B_v}X+\frac{\gamma_v}{B_v}\right)\right]^{-1/2} \tag{7}$$

$$Z = Y - 2 + \frac{4D_v}{B_v} X \tag{8}$$

We have used the definitions $Y = A_v/B_v$ and $X = (J+1/2)^2 - 1$; A_v, B_v, D_v, and Γ_v all have their customary meanings.

Since a linearly polarized laser was used in the experiments, the calculation that follows assumes linear polarization. The development for a circularly polarized laser would be similar. The scalar product of the molecular dipole moment and the electric field polarization is then [11–13, 20]

$$\bar{\mu} \cdot \hat{\varepsilon} = \sum_q D^{1\,*}_{0,q}(\varphi\theta\chi)\mu^1_q \tag{9}$$

where

$$\mu^1_q = \sum_n r_n Y_{1,q}(\hat{r}_n) \tag{10}$$

Here r_n is the position vector for the n^{th} electron in the molecular frame of reference and $Y_{1,q}(r_n)$ is a spherical harmonic. Using equations 2–5 and 9, equation 1 then becomes

$$\begin{aligned}
S_{gf} = \sum_{M_g M_f} \Bigg| & \sum_{\chi_i} \sum_{p_i N_i J_i M_i} \frac{1}{\omega_{ig} - \omega_{fg}/2 - i\Gamma_i/2} \\
& \left\langle \Phi_f 00 \middle| \frac{\langle \chi_f |}{\sqrt{2}} \left\{ \left\langle \tfrac{1}{2}\tfrac{1}{2} \middle| \left\langle J_f \tfrac{1}{2} M_f \right| \pm \left\langle \tfrac{1}{2} -\tfrac{1}{2} \middle| \left\langle J_f -\tfrac{1}{2} M_f \right| \right\} \right. \right. \\
& \sum_q D^{1\,*}_{0,q} \mu^1_q \frac{|\chi_i\rangle}{\sqrt{2}} \left\{ \alpha\left(\tfrac{1}{2}, N_i\right) \middle| \Phi_i 11 \right\rangle \middle| \tfrac{1}{2} -\tfrac{1}{2} \middle\rangle \middle| J_i \tfrac{1}{2} M_i \right\rangle + (-1)^{p_i} \alpha\left(\tfrac{1}{2}, N_i\right) \middle| \Phi_i 1 -1 \right\rangle \middle| \tfrac{1}{2}\tfrac{1}{2} \middle\rangle \middle| J_i -\tfrac{1}{2} M_i \right\rangle \\
& \quad + \alpha\left(\tfrac{3}{2}, N_i\right) \middle| \Phi_i 11 \right\rangle \middle| \tfrac{1}{2}\tfrac{1}{2} \middle\rangle \middle| J_i \tfrac{3}{2} M_i \right\rangle + (-1)^{p_i} \alpha\left(\tfrac{3}{2}, N_i\right) \middle| \Phi_i 1 -1 \right\rangle \middle| \tfrac{1}{2} -\tfrac{1}{2} \middle\rangle \middle| J_i -\tfrac{3}{2} M_i \right\rangle \Big\} \\
& \frac{\langle \chi_i |}{\sqrt{2}} \left\{ \alpha\left(\tfrac{1}{2}, N_i\right) \langle \Phi_i 11 \middle| \left\langle \tfrac{1}{2} -\tfrac{1}{2} \middle| \left\langle J_i \tfrac{1}{2} M_i \right| + (-1)^{p_i} \alpha\left(\tfrac{1}{2}, N_i\right) \langle \Phi_i 1 -1 \middle| \left\langle \tfrac{1}{2}\tfrac{1}{2} \middle| \left\langle J_i -\tfrac{1}{2} M_i \right| \right. \right. \right. \\
& \quad + \alpha\left(\tfrac{3}{2}, N_i\right) \langle \Phi_i 11 \middle| \left\langle \tfrac{1}{2}\tfrac{1}{2} \middle| \left\langle J_i \tfrac{3}{2} M_i \right| + (-1)^{p_i} \alpha\left(\tfrac{3}{2}, N_i\right) \langle \Phi_i 1 -1 \middle| \left\langle \tfrac{1}{2} -\tfrac{1}{2} \middle| \left\langle J_i -\tfrac{3}{2} M_i \right| \right\} \\
& \left. \left. \sum_{q'} D^{1\,*}_{0,q'} \mu^1_{q'} \middle| \Phi_g 00 \right\rangle \frac{|\chi_g\rangle}{\sqrt{2}} \left\{ \left| \tfrac{1}{2}\tfrac{1}{2} \right\rangle \middle| J_g \tfrac{1}{2} M_g \right\rangle \pm \left| \tfrac{1}{2} -\tfrac{1}{2} \right\rangle \middle| J_g -\tfrac{1}{2} M_g \right\rangle \Big\} \Bigg|^2
\end{aligned} \tag{11}$$

Index p_i assumes the values 0 and 1; index N_i varies between J_i -1/2 and J_i +1/2. The dipole moment operator defined in equation 10 does not affect the electron spin wavefunctions $|S\Sigma\rangle$. Therefore, only those terms with $\Sigma g = \Sigma i = \Sigma f$ survive. Rotational matrix elements are evaluated using [16]

$$\langle J'\,\Omega'\,M'|D^{1\,*}_{0,q}\,|J\Omega M\rangle = \frac{[(2J'+1)(2J+1)]^{1/2}}{8\pi^2}\int D^{J'}_{M',\Omega'} D^{1\,*}_{0,q}\, D^{J\,*}_{M,\Omega}\, d\tau$$

$$= (-1)^{M'-\Omega'}[(2J'+1)(2J+1)]^{1/2}\begin{pmatrix} J & 1 & J' \\ M & 0 & -M' \end{pmatrix}\begin{pmatrix} J & 1 & J' \\ \Omega & q & -\Omega' \end{pmatrix} \qquad (12)$$

The properties of the Wigner 3j coefficients then require $M_g = M_i = M_f = M$ in equation 11. Furthermore, for fixed Ω_i and Ω_g, or Ω_f and Ω_i, the second 3j coefficient in equation 12 selects only a single term in the sums over q and q'. Equation 11 then reduces to

$$S_{gf} = \frac{(2J_f+1)(2J_g+1)}{16}\sum_M \left|\sum_{\chi_i}\langle\chi_f|\chi_i\rangle\langle\chi_i|\chi_g\rangle\right.$$

$$\sum_{p_i N_i J_i}\frac{2J_i+1}{\omega_{ig}-\omega_{fg}/2-i\Gamma_i/2}\begin{pmatrix} J_i & 1 & J_f \\ M & 0 & -M \end{pmatrix}\begin{pmatrix} J_g & 1 & J_i \\ M & 0 & -M \end{pmatrix}$$

$$\left\{(-1)^{p_i}\alpha\left(\tfrac{1}{2},N_i\right)\langle\Phi_f 00|\mu^1_1|\Phi_i 1-1\rangle\begin{pmatrix} J_i & 1 & J_f \\ -1/2 & 1 & -1/2 \end{pmatrix} + \alpha\left(\tfrac{3}{2},N_i\right)\langle\Phi_f 00|\mu^1_{-1}|\Phi_i 11\rangle\begin{pmatrix} J_i & 1 & J_f \\ 3/2 & -1 & -1/2 \end{pmatrix}\right.$$

$$\left. \mp\,\alpha\left(\tfrac{1}{2},N_i\right)\langle\Phi_f 00|\mu^1_{-1}|\Phi_i 11\rangle\begin{pmatrix} J_i & 1 & J_f \\ 1/2 & -1 & 1/2 \end{pmatrix} \mp (-1)^{p_i}\alpha\left(\tfrac{3}{2},N_i\right)\langle\Phi_f 00|\mu^1_1|\Phi_i 1-1\rangle\begin{pmatrix} J_i & 1 & J_f \\ -3/2 & 1 & 1/2 \end{pmatrix}\right\}$$

$$\left\{(-1)^{p_i}\alpha\left(\tfrac{1}{2},N_i\right)\langle\Phi_i 1-1|\mu^1_{-1}|\Phi_g 00\rangle\begin{pmatrix} J_g & 1 & J_i \\ 1/2 & -1 & 1/2 \end{pmatrix} + \alpha\left(\tfrac{3}{2},N_i\right)\langle\Phi_i 11|\mu^1_1|\Phi_g 00\rangle\begin{pmatrix} J_g & 1 & J_i \\ 1/2 & 1 & -3/2 \end{pmatrix}\right.$$

$$\left.\left. \mp\,\alpha\left(\tfrac{1}{2},N_i\right)\langle\Phi_i 11|\mu^1_1|\Phi_g 00\rangle\begin{pmatrix} J_g & 1 & J_i \\ -1/2 & 1 & -1/2 \end{pmatrix} \mp (-1)^{p_i}\alpha\left(\tfrac{3}{2},N_i\right)\langle\Phi_i 1-1|\mu^1_{-1}|\Phi_g 00\rangle\begin{pmatrix} J_g & 1 & J_i \\ -1/2 & -1 & 3/2 \end{pmatrix}\right\}\right|^2 \qquad (13)$$

We evaluate the relative signs of the electronic transition moments using the Wigner-Eckert theorem [16],

$$\langle \Phi' L' \Lambda' | \mu_q^1 | \Phi L \Lambda \rangle = (-1)^{L'-\Lambda'} \begin{pmatrix} L' & 1 & L \\ -\Lambda' & q & \Lambda \end{pmatrix} \langle \Phi' L' \| \mu^1 \| \Phi L \rangle \tag{14}$$

which yields

$$\langle \Phi_f 00 | \mu_1^1 | \Phi_i 1 -1 \rangle = \langle \Phi_f 00 | \mu_{-1}^1 | \Phi_i 11 \rangle = \frac{\langle \Phi_f 0 \| \mu^1 \| \Phi_i 1 \rangle}{\sqrt{3}} = \frac{\langle \mu \rangle}{\sqrt{3}}$$

and

$$\langle \Phi_i 11 | \mu_1^1 | \Phi_g 00 \rangle = \langle \Phi_i 1 -1 | \mu_{-1}^1 | \Phi_g 00 \rangle = \frac{\langle \Phi_i 1 \| \mu^1 \| \Phi_g 0 \rangle}{\sqrt{3}} = \frac{\langle \mu' \rangle}{\sqrt{3}} \tag{15}$$

In each bracket in equation 13, there are only two unique 3j symbols. We choose to convert those having $(-1)^{pi}$ cofactors by changing the signs of each parameter in the bottom row. This operation introduces phase factors $(-1)^{J_i+J_f+1}$ and $(-1)^{J_g+J_i+1}$, which are equivalent to $(-1)^{\Delta J + p_i}$ and $(-1)^{\Delta J' + p_i}$, where $\Delta J = J_f - J_i$ and $\Delta J' = J_i - J_g$. The line strength can then be written as

$$S_{gf} = \frac{(2J_f+1)(2J_g+1)}{144} \langle \mu \rangle^2 \langle \mu' \rangle^2 \sum_M \left| \sum_{\chi_i} \langle \chi_f | \chi_i \rangle \langle \chi_i | \chi_g \rangle \right.$$

$$\sum_{p_i N_i J_i} \frac{2J_i+1}{\omega_{ig} - \omega_{fg}/2 - i\Gamma_i/2} \begin{pmatrix} J_i & 1 & J_f \\ M & 0 & -M \end{pmatrix} \begin{pmatrix} J_g & 1 & J_i \\ M & 0 & -M \end{pmatrix}$$

$$\left\{ \left[(-1)^{\Delta J + p_i} \mp 1 \right] \alpha\left(\tfrac{1}{2}, N_i\right) \begin{pmatrix} J_i & 1 & J_f \\ 1/2 & -1 & 1/2 \end{pmatrix} + \left[1 \mp (-1)^{\Delta J + p_i} \right] \alpha\left(\tfrac{3}{2}, N_i\right) \begin{pmatrix} J_i & 1 & J_f \\ 3/2 & -1 & -1/2 \end{pmatrix} \right\}$$

$$\left. \left\{ \left[(-1)^{\Delta J' + p_i} \mp 1 \right] \alpha\left(\tfrac{1}{2}, N_i\right) \begin{pmatrix} J_g & 1 & J_i \\ -1/2 & 1 & -1/2 \end{pmatrix} + \left[1 \mp (-1)^{\Delta J' + p_i} \right] \alpha\left(\tfrac{3}{2}, N_i\right) \begin{pmatrix} J_g & 1 & J_i \\ 1/2 & 1 & -3/2 \end{pmatrix} \right\} \right|^2 \tag{16}$$

The upper (lower) sign is chosen in the first bracket for F_1 (F_2) levels of the final $B^2\Sigma^+$ state ($|f\rangle$). A similar choice is made to select the F_1 or F_2 levels of the ground $X^2\Sigma^+$ state ($|g\rangle$) in the second bracket. Parity and ΔJ selection rules are obvious in this final expression. In particular, equation 16 allows six main and four satellite branches: O_1, O_2, Q_1, Q_2, S_1, S_2, $^QP_{21}$, $^OP_{12}$, $^SR_{21}$, and $^QR_{12}$.

4. RESULTS AND DISCUSSION

In the $B^2\Sigma^+ \leftarrow X^2\Sigma^+$ (3,0) spectrum, the laser detuning from resonance ($|\omega_{ig} - \omega_{fg}/2|$) was always much greater than the natural linewidths ($\approx 10^{-6}$ cm^{-1}); therefore, to simplify the calculation, Γ_i was neglected in the line-strength calculation. However, because the laser linewidth is finite and the $A^2\Pi_i$–$X^2\Sigma^+$ transitions saturate when the energy per pulse is less than a millijoule, this assumption may not be wholly valid for all lines. The only intermediate vibrational level used in the calculation is the $A^2\Pi_i$ v′=4 level. Thus, the sum over vibrational integrals collapses to a single term, $\langle\chi_3|\chi_4\rangle\langle\chi_4|\chi_0\rangle$.

Constants for the $X^2\Sigma^+$, v″=0 and $A^2\Pi_i$, v′=4 levels were taken from Kotlar et al. [21]. The term value (E) for $A^2\Pi_i$, v′=4 was computed from the Dunham expansion for vibrational levels. Spectroscopic constants for the $B^2\Sigma^+$, v′=3 vibronic state were taken from Ito et al. [22]. Constants for all three states are listed in Table 1. The constants for the $X^2\Sigma^+$ and $A^2\Pi_i$ states were used to compute wavelengths for $A^2\Pi_i \leftarrow X^2\Sigma^+$ (4,0) LIF spectra obtained in a flame [7]. Calculated wavelengths matched the experimental results within the laser bandwidth.

Calculations using equation 16 have shown that if the varying contribution of the term $1/(\omega_{ig} - \omega_{fg}/2 - i\Gamma_f/2)$ is ignored, the reduced line strengths $S_{gf}/(2J_g+1)$ of the Q_1- and Q_2-branches are the same for a given J_g, and the same is true for the O-, P-, R-, and S-branches. As expected for linear polarization, the Q-branch lines are much stronger than the O- and S-branch lines for this $\Delta\Omega$=0 two-photon transition [8, 9, 13]. The Q-branch reduced line strengths are nearly constant for large J_g [8–11]. The P- and R-branch line strengths decrease rapidly with increasing J_g.

The results of the calculation, with computed detunings, are compared to the experimental spectrum in Figure 1. Line strengths were computed up to $J_g = 30.5$. Because the rotational B constants of the $B^2\Sigma^+$ and $X^2\Sigma^+$ states are nearly identical (see Table 1), the spectrum has a line-like Q-branch with headless O- and S-branches. The latter have very evenly spaced lines.

Table 1. Spectroscopic Constants Used in the Calculation of Two-Photon Line Strengths for the CN $B^2\Sigma^+ - X^2\Sigma^+$ (3,0) Band. (All symbols have their usual spectroscopic definitions. Constants are taken from Kotlar et al. [21] and Ito et al. [22] and are expressed in units of centimeters^{-1}.)

	$X^2\Sigma^+$, v=0	$B^2\Sigma^+$, v=3	$A^2\Pi_i$, v=4
E ($\times 10^{-4}$)	0.0	3.2045917	1.611475500
B	1.891077896	1.89417	1.637882921
D ($\times 10^{6}$)	6.406535208	7.0268	6.128776498
γ ($\times 10^{2}$)	0.7254551000	2.22	—
H ($\times 10^{12}$)	6.331907154	-11.8	—
γ_D ($\times 10^{8}$)	-1.814133463	-87.6	—
γ_H ($\times 10^{12}$)	—	-9.8	—
A	—	—	-52.32744572
q ($\times 10^{4}$)	—	—	-4.117828087
p ($\times 10^{3}$)	—	—	7.628636855
α	—	—	-3.85102
β ($\times 10^{2}$)	—	—	2.0818
p_D ($\times 10^{7}$)	—	—	1.975351405

The $O_1(J_g)$, $O_2(J_g - 1)$, and $^{O}P_{12}(J_g - 1)$ transitions are unresolved as are the $S_1(J_g)$, $S_2(J_g - 1)$, and $^{S}R_{21}(J_g)$ lines. The Q_1-, Q_2-, $^{Q}P_{21}$-, and $^{Q}P_{12}$-branches all contribute to the strong, sharp feature near 623.9 nm. The simulated spectrum is a least-squares fit to the measured spectrum, obtained by varying only the temperature and a scaling factor. The Q-branch is not included in the fit for reasons that are discussed in the following paragraph. The effective transition linewidth is fixed at 0.9 cm^{-1}.

The ground-state rotational-distribution temperature that produces the best fit is 150 K. It should be explicitly noted that the expected rotational distribution in the ground state is that

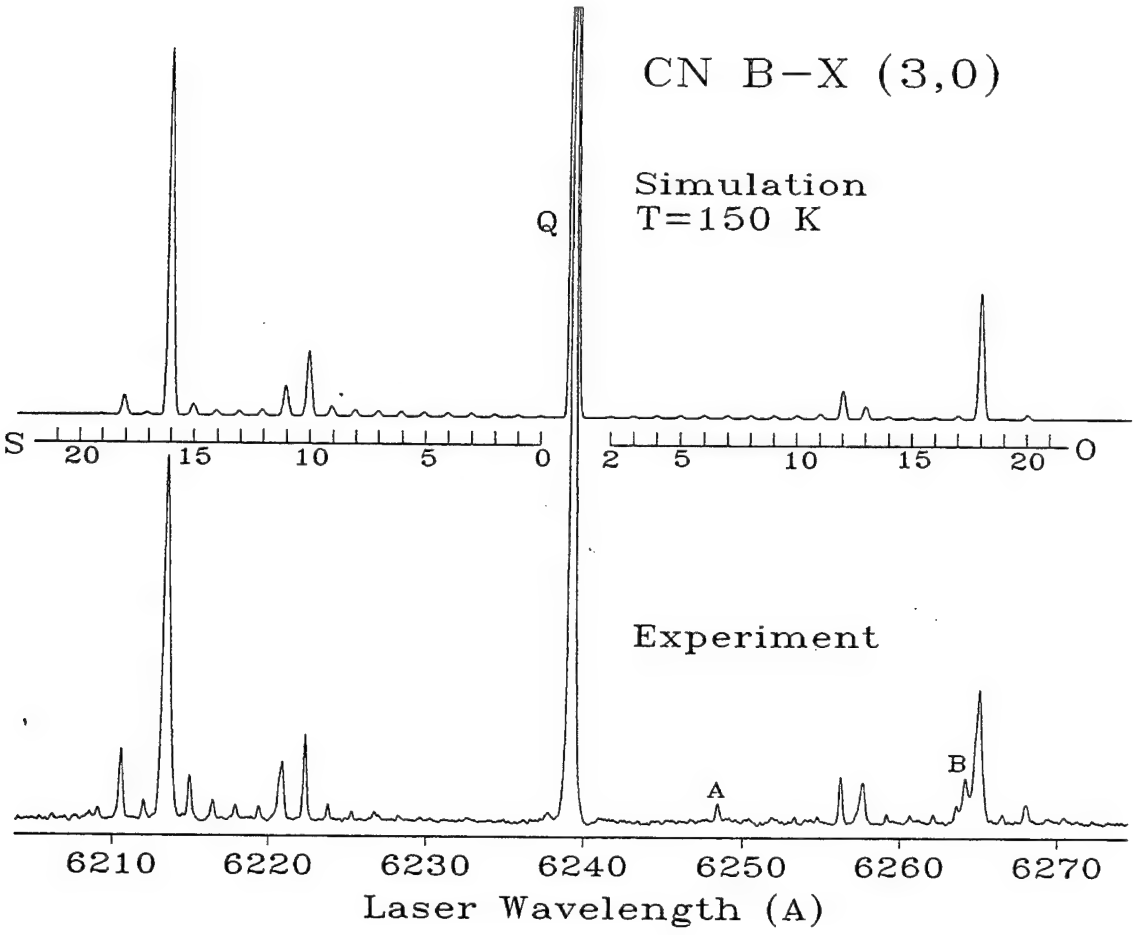

Figure 1. Comparison of a simulated spectrum using the computed line strengths with the observed spectrum. The temperature for the simulation is 150 K. Only the temperature and a scale factor were varied in the simulation to best fit the experimental spectrum. Features A and B are discussed in the text.

characterized by an equilibrated population at 300 K. This unexpected difference is not well understood. Several possible systematic measurement errors were considered and dismissed. (1) The transmission bandpass of the detection filter was wide enough so that the filter/PMT combination was equally sensitive to fluorescence from all of the transitions observed in the $B^2\Sigma^+$-$X^2\Sigma^+$ (3,3) band. (2) Variation in the laser intensity over the wavelength region scanned was very small. In any case, a systematic variation of the laser intensity would cause a monotonically varying discrepancy from the violet to red ends of the spectrum. However, the discrepancy for a 300-K simulation is not monotonic because low *N* transitions occur in the O-

and S-branches near the *center* of the band, while high N transitions are in the *wings* (see Figure 1). (3) The pressure was low enough that collisional effects in the excited $B^2\Sigma^+$ state, which can strongly affect temperatures measured by LIF rotational excitation scans [24, 25], are not believed to be of any consequence. (4) Self-absorption of the emitted radiation by ground-state molecules is of no consequence since the emission is mainly due to a high-lying vibrational level (v″=3).

Because the Q-branch is unresolved and many of its lines are saturated in the measured spectrum [7], no attempt was made to fit its intensity; the simulated Q-branch at 150 K is about 80% stronger than that measured. The simulation reproduces the major features of the $B^2\Sigma^+$–$X^2\Sigma^+$ (3,0) band two-photon absorption spectrum. Discrepancies may be at least partially attributed to saturation of the stronger transitions in the measured spectrum considering that the line strengths vary over several orders of magnitude. Especially for transitions where the intermediate state detuning is less than a wave number, it is probable that the intermediate $A^2\Pi_i$ – $X^2\Sigma^+$ transition is saturated, and neglect of the $i\Gamma_i'$ term in the energy denominator is not justified.

For each transition in the 10 branches, there are particular pathways from the $X^2\Sigma^+$ to the $B^2\Sigma^+$ state that involve dipole-allowed quasi-resonant transitions in the $A^2\Pi_i$ – $X^2\Sigma^+$ (4,0) band followed by a second dipole-allowed transition in the $B^2\Sigma^+$–$A^2\Pi_i$ (3,4) band. These pathways are schematically indicated in Figure 2 for the O_1-, $^QP_{21}$-, and Q_1-branches. The O- and S-branch transitions each have two possible allowed pathways, the P- and R-satellite-branch transitions have four possible pathways, and the Q-branch transitions have six possible pathways. When the photon energy is nearly resonant with any one of the allowed transitions in the $A^2\Pi_i$ – $X^2\Sigma^+$ (4,0) band for a given $B^2\Sigma^+$–$X^2\Sigma^+$ (3,0) line, an enhancement in the line strength is expected. In Figure 3 the magnitude of the detuning ($|\omega_{ig} - \omega_{fg}/2|$) is plotted as a function of N_g for the six $\Delta N \neq 0$ branches in a particular path. Comparison with Figure 1 shows that the values of N_g for which the single-photon detuning is small are those for which a strong two-photon absorption occurs in a particular branch. The reduced intensity of O(20) relative to O(18) and of S(18) relative to S(16) is due to the differences in the detuning between these pairs of lines, which is

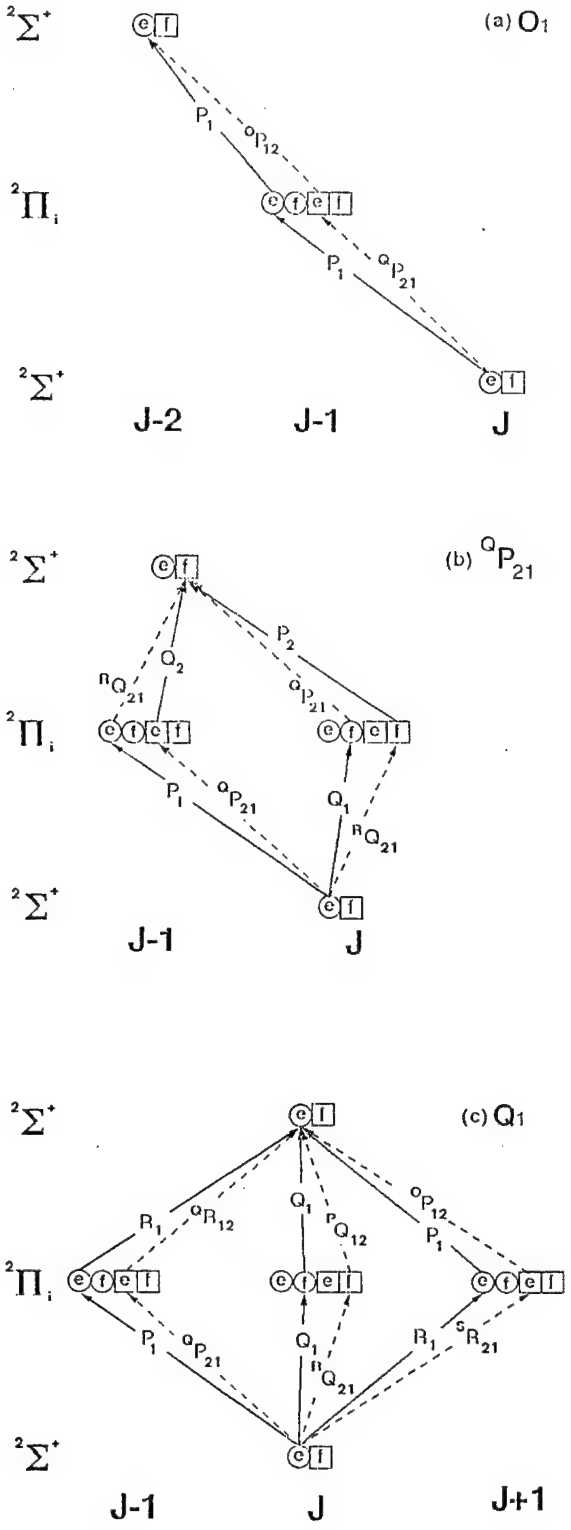

Figure 2. Schematic illustration of allowed one-photon pathways for a $^2\Sigma^+$–$^2\Sigma^+$ two-photon transition through a $^2\Pi_i$ intermediate state. F_1 levels are symbolized by circles; F_2 levels by squares; and e/f indicates the parity of the level. (a) O_1 transitions; (b) $^{Q}P_{21}$ transitions; (c) Q_1 transitions.

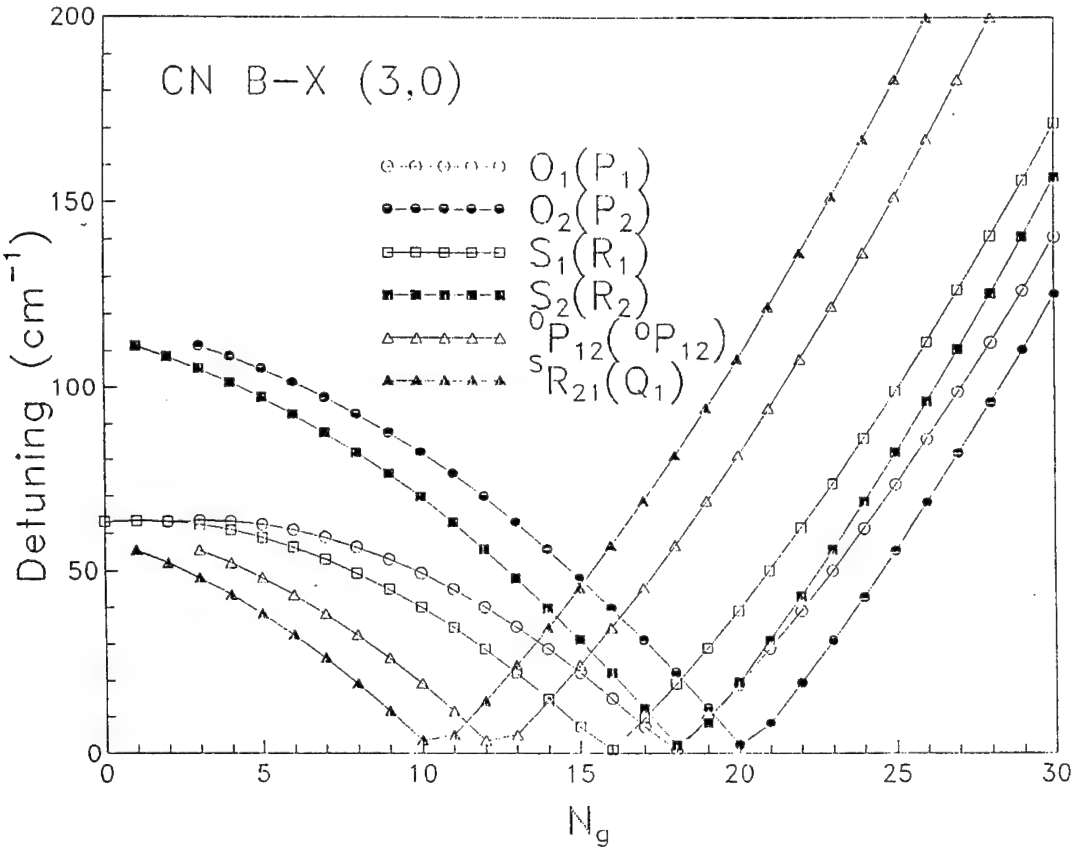

Figure 3. Detuning of the laser from resonance ($|\omega_{ig} - \omega_{fg}/2|$) plotted as a function of the ground-state quantum number N_g for a particular pathway in each of the six $\Delta N \neq 0$ branches. The $A^2\Pi_i \leftarrow X^2\Sigma^+$ (4,0) branch that provides the first step of the selected pathway is indicated in parentheses for each two-photon branch.

roughly a factor of 2.5, and a (modeled) difference in the Boltzmann distribution of the ground-state levels.

The striking near-symmetry in the peak intensities relative to reflection of the spectrum about the Q-branch is, again, related to the similarity of the rotational constants for $B^2\Sigma^+$, v′=3 and $X^2\Sigma^+$, v″=0 levels. For example, the strongest O- and S-branch transitions are O_1 (18.5) and S_1(16.5). Both transitions are enhanced by a single-photon near resonance with the same intermediate level in the $A^2\Pi_i$, v′=4 level: Ω=3/2, J_i=17.5, e parity. The similarity of the rotational constants means that the energy gap between J_g = 16.5 and J_g = 18.5 is almost exactly the same as that between J_f = 16.5 and J_f = 18.5. Therefore, whatever the detuning is for the near resonant intermediate level (J_i = 17.5 in this case) for the O_1 (18.5) line, it must be closely

matched by the detuning for the S_1 (16.5) line. A similar relationship holds for all of the pairs $O_2(J_g)$ and $S_2(J_g\text{-}2)$ and likewise for the pairs $^{O}P_{12}(J_g)$ and $^{S}R_{21}(J_g\text{-}1)$. The same intermediate state contributes to the absorption, and the detuning is almost the same for both lines in a pair. Thus, resonantly enhanced peaks appear symmetrically about the strong Q-branch. The assumed rotational distribution (T=150 K) in the $X^2\Sigma^+$, v″=0 vibronic level accounts for the fact that the related peaks are less intense to the red side of the Q-branch than to the blue.

Most of the peaks in the measured spectrum show a degree of asymmetry. In particular, the strong O(13) and S(11) peaks clearly have a wing to the blue. This asymmetry is not an experimental artifact. The intensity enhancement for both peaks is dominated by $^{O}P_{12}(12.5)$ and $^{S}R_{21}(11.5)$ contributions due to a near resonance with the same intermediate level: Ω=3/2, J_i=11.5, f parity. The asymmetry is not due to a perturbation of the intermediate level. The $A^2\Pi_i$, v′=4 level has no perturbations (due to $X^2\Sigma^+$, v=8) below J = 50.5 [21]. Moreover, since the strongest lines (with the closest intermediate resonance) are those that appear most asymmetric, these asymmetries may be due to the AC Stark effect [26].

Two anomalous peaks appear within the two-photon spectrum, labeled A and B in Figure 1. Peak A is very likely the Q-branch of the $B^2\Sigma^+$–$X^2\Sigma^+$ (4,1) band. The wave number of the peak (≈31,999 cm^{-1}) is that expected for the origin of the (4,1) band [6]. This hot band is also characterized by nearly identical values of the rotational constants in the upper and lower states [22, 27], giving rise to a strong feature at the band origin. The observation of the (4,1) band is doubly unexpected because of its poor Franck-Condon factor and the absence of a near-resonant intermediate state [6]. However, because about 20% of the CN molecules produced by photolysis have v″=1, there is a sizable population available for two-photon absorption. We have been unable to identify the feature labeled B in Figure 1. The energy of the transition precludes it being another $B^2\Sigma^+$–$X^2\Sigma^+$, Δv=3 Q-branch, and, in any case, no vibrational level higher than v″=1 in the ground state is expected to be significantly populated. Peak B is also not due to a single-color, collision-assisted double resonance absorption [7]. Rotational levels that would promote this process are not available in the $A^2\Pi_i$, v=4 vibronic level at half the energy of anomalous peak B.

5. SUMMARY

This work reports observation of a unique set of two-photon absorptions in the CN $B^2\Sigma^+ \leftarrow X^2\Sigma^+$ (3,0) band, wherein several $A^2\Pi_i$, $v'=4$ rovibronic levels provide near-resonant enhancement of many two-photon transitions. A calculation of the line strength for such a transition using angular momentum formalism reproduces the major features of the observed spectrum. Discrepancies may be due to saturation of transitions in the experiment, errors in the spectroscopic constants used to calculate the line strengths, or unjustified neglect of the laser bandwidth relative to the transition detunings. The discovery of this near-resonant two-photon transition with its well-developed rotational branches opens several possibilities as tests of multiple-photon absorption theory. The system clearly merits further study. An obvious experiment would be to excite the Q-head of the transition and attempt to resolve the $B^2\Sigma^+ \rightarrow X^2\Sigma^+$ (3,3) R-branch fluorescence. This experiment would provide a test of the computed relative intensities in the Q-head absorption. In addition, an attempt to measure the absolute intensities of the absorptions could be revealing. Use of a narrow bandwidth laser or two-color experiments could also be extremely enlightening. Finally, the transition could prove an excellent test of theories of polarization and the AC Stark effect [26].

INTENTIONALLY LEFT BLANK.

6. REFERENCES

1. Woerdman, J. P. "Polarization Dependence of Near-Resonant Two-Photon Absorption of Na_2 Vapor." Chem. Phys. Lett., vol. 50, p. 41, 1977.

2. Woerdman, J. P. "New Doppler-Free Two-Photon Lines in High-Density Sodium Vapor." Opt. Commun., vol. 18, p. 223, 1976.

3. Woerdman, J. P. "Doppler-Free Two-Photon Transitions of the Sodium Molecule." Chem. Phys. Lett., vol. 43, p. 279, 1976.

4. Woerdman, J. P., and M. F. H. Shuurmans. Doppler-Free Three-Photon Cross-Resonances in Na_2 Vapor." Opt. Commun., vol. 21, p. 243, 1977.

5. Tjossem, P., J. H. Paul, K. C. Smyth. "Multiphoton Ionization Detection of CH, Carbon Atoms, and O_2 in Premixed Hydrocarbon Flames." Chem. Phys. Lett., vol. 144, p. 51, 1988.

6. Knowles, P. J., H. Werner, P. J. Hay, and D. C. Cartwright. "The $A^2\Pi$-$X^2\Sigma^+$ Red and $B^2\Sigma^+$-$X^2\Sigma^+$ Violet Systems of the CN Radical: Accurate Multireference Configuration Interaction Calculations of the Radiative Transition Probabilities." J. Chem. Phys., vol. 89, p. 7334, 1988.

7. Guthrie, J. A., T. S. Bowen, W. R. Anderson, A. J. Kotlar, and S. W. Bunte. "Unique One- and Two-Photon Absorption Processes Near 6000 Å in Nascent CN in a Flame. Direct and Collision—Assisted Population of the $B^2\Sigma^+$ Electronic State." Chem. Phys., vol. 175, p. 343, 1993; J. A. Guthrie, T. S. Bowen, W. R. Anderson, A. J. Kotlar, and S. W. Bunte. "Unusual Laser Excitation (5890–6520 Å) of the $B^2\Sigma^+$ Electronic State of CN in an Atmospheric Pressure Flame." ARL Technical Report, in press.

8. Bray, R. G., and R. M. Hochstrasser. "Two-Photon Absorption by Rotating Diatomic Molecules." Mol. Phys., vol. 31, p. 412, 1976.

9. Chen, K., and E. S. Yeung. "Rovibronic Two-Photon Excitations of Symmetric Top Molecules." J. Chem. Phys., vol. 69, p. 43, 1978.

10. Metz, F., W. E. Howard, L. Wunsch, H. J. Neusser, and E. W. Schlag. "The Theory of Molecular Two-Photon Spectroscopy in the Gas Phase." Proc. Roy. Soc., London A, vol. 363, p. 381, 1978.

11. Kummel, A. C., G. O. Sitz, and R. N. Zare. "Determination of Population and Alignment of the Ground State Using Two-Photon Nonresonant Excitation." J. Chem. Phys., vol. 85, p. 6874, 1986.

12. Mainos, C., M. C. Castex, and H. Nkwawo. "Hund's Coupling Case Sequences in Resonant Multiphoton Transitions." J. Chem. Phys., vol. 93, p. 5370, 1990.

13. Halpern, J. B., H. Zacharias, and R. Wallenstein. "Rotational Line Strengths in Two- and Three-Photon Transitions in Diatomic Molecules." J. Mol. Spectrosc., vol. 79, p. 1, 1980.

14. Halpern, J. B., and W. M. Jackson. "Energy Partitioning in the Dissociation of Cyanogen at 193 nm." J. Phys. Chem., vol. 86, p. 973, 1982.

15. Bebb, H., and A. Gold. "Multiphoton Ionization of Hydrogen and Rare Gas Atoms." Phy. Rev., vol. 143, p. 1, 1966.

16. Zare, R. N. Angular Momentum. New York: J. Wiley and Sons, 1988.

17. Hougen, J. T. "The Calculation of Rotational Energy Levels and Rotational Line Intensities in Diatomic Molecules." (USA) National Bureau of Standards Momograph, vol. 115, 1970.

18. Alexander, M. H., and P. J. Dagdigian. "Clarification of the Electronic Assymetry in Π State Λ Doublets with Some Implications for Molecular Collisions." J. Chem. Phys., vol. 80, p. 4325, 1984.

19. Bennett, R. J. M. "Honl-London Factors for Doublet Transitions in Diatomic Molecules." Mon. Not. Roy. Astronom. Soc., vol. 147, p. 35, 1970.

20. Jacobs, D. C., and R. N. Zare. "Reduction of 1+1 Resonance Enhanced MPI Spectra to Populations and Alignment Factors." J. Chem. Phys., vol. 85, p. 5457, 1986.

21. Kotlar, A. J., R. W. Field, J. I. Steinfeld, and J. A. Coxon. "Analysis of Perturbations in the $A^2\Pi$-$X^2\Sigma^+$ "Red" System of CN." J. Mol. Spectrosc., vol. 80, p. 86, 1980, and supplementary material.

22. Ito, H., Y. Ozaki, K. Suzuki, T. Kondow, and K. Kuchitsu. "Analysis of the $B^2\Sigma^+$~$A^2\Pi_i$ Perturbations in the CN ($B^2\Sigma^+$-$X^2\Sigma^+$) Main Band System." J. Mol. Spectrosc., vol. 127, p. 283, 1988.

23. Tjossem, P. J. H., and K. C. Smyth. "Multiphoton Excitation Spectroscopy of the $B^1\Sigma^+$ and $C^1\Sigma$+ Rydberg States of CO." J. Chem. Phys., vol. 91, p. 2041, 1989.

24. Crosley, D. R. "Collisional Effects on Laser-Induced Fluorescence Flame Measurements." Opt. Eng., vol. 20, p. 511, 1981.

25. Crosley, D. R., and G. P. Smith. "Laser-Induced Fluorescence Spectroscopy for Combustion Diagnostics." Opt. Eng., vol. 22, p. 545, 1983.

26. Girard, B., G. O. Sitz, R. N. Zare, N. Billy, and J. Vigue. "Polarization Dependence of the AC Stark Effect in Multiphoton Transitions of Diatomic Molecules." J. Chem. Phys., vol. 97, p. 26, 1992.

27. Engleman, R. "The $A_v = 0$ and +1 Sequence Bands of the CN Violet System Observed During the Flash Photolysis of BrCN." J. Mol. Spectrosc., vol. 49, p. 106, 1974.

INTENTIONALLY LEFT BLANK.

NO. OF COPIES	ORGANIZATION
2	DEFENSE TECHNICAL INFORMATION CENTER DTIC DDA 8725 JOHN J KINGMAN RD STE 0944 FT BELVOIR VA 22060-6218
1	HQDA DAMO FDQ DENNIS SCHMIDT 400 ARMY PENTAGON WASHINGTON DC 20310-0460
1	CECOM SP & TRRSTRL COMMCTN DIV AMSEL RD ST MC M H SOICHER FT MONMOUTH NJ 07703-5203
1	PRIN DPTY FOR TCHNLGY HQ US ARMY MATCOM AMCDCG T M FISETTE 5001 EISENHOWER AVE ALEXANDRIA VA 22333-0001
1	PRIN DPTY FOR ACQUSTN HQS US ARMY MATCOM AMCDCG A D ADAMS 5001 EISENHOWER AVE ALEXANDRIA VA 22333-0001
1	DPTY CG FOR RDE HQS US ARMY MATCOM AMCRD BG BEAUCHAMP 5001 EISENHOWER AVE ALEXANDRIA VA 22333-0001
1	ASST DPTY CG FOR RDE HQS US ARMY MATCOM AMCRD COL S MANESS 5001 EISENHOWER AVE ALEXANDRIA VA 22333-0001

NO. OF COPIES	ORGANIZATION
1	DPTY ASSIST SCY FOR R&T SARD TT F MILTON THE PENTAGON RM 3E479 WASHINGTON DC 20310-0103
1	DPTY ASSIST SCY FOR R&T SARD TT D CHAIT THE PENTAGON WASHINGTON DC 20310-0103
1	DPTY ASSIST SCY FOR R&T SARD TT K KOMINOS THE PENTAGON WASHINGTON DC 20310-0103
1	DPTY ASSIST SCY FOR R&T SARD TT B REISMAN THE PENTAGON WASHINGTON DC 20310-0103
1	DPTY ASSIST SCY FOR R&T SARD TT T KILLION THE PENTAGON WASHINGTON DC 20310-0103
1	OSD OUSD(A&T)/ODDDR&E(R) J LUPO THE PENTAGON WASHINGTON DC 20301-7100
1	INST FOR ADVNCD TCHNLGY THE UNIV OF TEXAS AT AUSTIN PO BOX 202797 AUSTIN TX 78720-2797
1	DUSD SPACE 1E765 J G MCNEFF 3900 DEFENSE PENTAGON WASHINGTON DC 20301-3900
1	USAASA MOAS AI W PARRON 9325 GUNSTON RD STE N319 FT BELVOIR VA 22060-5582

NO. OF COPIES ORGANIZATION

1 CECOM
PM GPS COL S YOUNG
FT MONMOUTH NJ 07703

1 GPS JOINT PROG OFC DIR
COL J CLAY
2435 VELA WAY STE 1613
LOS ANGELES AFB CA 90245-5500

1 ELECTRONIC SYS DIV DIR
CECOM RDEC
J NIEMELA
FT MONMOUTH NJ 07703

3 DARPA
L STOTTS
J PENNELLA
B KASPAR
3701 N FAIRFAX DR
ARLINGTON VA 22203-1714

1 SPCL ASST TO WING CMNDR
50SW/CCX
CAPT P H BERNSTEIN
300 O'MALLEY AVE STE 20
FALCON AFB CO 80912-3020

1 USAF SMC/CED
DMA/JPO
M ISON
2435 VELA WAY STE 1613
LOS ANGELES AFB CA 90245-5500

1 US MILITARY ACADEMY
MATH SCI CTR OF EXCELLENCE
DEPT OF MATHEMATICAL SCI
MDN A MAJ DON ENGEN
THAYER HALL
WEST POINT NY 10996-1786

1 DIRECTOR
US ARMY RESEARCH LAB
AMSRL CS AL TP
2800 POWDER MILL RD
ADELPHI MD 20783-1145

NO. OF COPIES ORGANIZATION

1 DIRECTOR
US ARMY RESEARCH LAB
AMSRL CS AL TA
2800 POWDER MILL RD
ADELPHI MD 20783-1145

3 DIRECTOR
US ARMY RESEARCH LAB
AMSRL CI LL
2800 POWDER MILL RD
ADELPHI MD 20783-1145

ABERDEEN PROVING GROUND

2 DIR USARL
AMSRL CI LP (305)

NO. OF COPIES	ORGANIZATION
1	DEPT OF PHYSICS UNIV OF CENTRAL OKLAHOMA ATTN J A GUTHRIE EDMOND OK 73034
2	CTR FOR THE STUDY OF TERRESTRIAL AND EXTRATERRESTRIAL ATMOSPHERES HOWARD UNIVERSITY ATTN YUHUI HUANG JOSHUA B HALPERN WASHINGTON DC 20059

NO. OF COPIES	ORGANIZATION
	ABERDEEN PROVING GROUND
39	DIR, USARL ATTN: AMSRL-WM-P, A. W. HORST AMSRL-WM-PC, B. E. FORCH G. F. ADAMS W. R. ANDERSON R. A. BEYER S. W. BUNTE C. F. CHABALOWSKI K. P. MC-NEILL BOONSTOPPEL A. COHEN R. DANIEL D. DEVYNCK R. A. FIFER J. M. HEIMERL B. E. HOMAN A. JUHASZ A. J. KOTLAR R. KRANZE E. LANCASTER W. F. MCBRATNEY K. L. MCNESBY M. MCQUAID N. E. MEAGHER M. S. MILLER A. W. MIZIOLEK J. B. MORRIS J. E. NEWBERRY W. V. PAI R. A. PESCE-RODRIGUEZ J. RASIMAS B. M. RICE P. SAEGAR R. C. SAUSA M. A. SCHROEDER R. SCHWEITZER L. D. SEGER J. A. VANDERHOFF D. VENIZELOS W. WHREN H. L. WILLIAMS

INTENTIONALLY LEFT BLANK.

REPORT DOCUMENTATION PAGE

Form Approved OMB No. 0704-0188

1. AGENCY USE ONLY *(Leave blank)*	2. REPORT DATE	3. REPORT TYPE AND DATES COVERED
	June 1997	Final, January 1991 - December 1996

4. TITLE AND SUBTITLE

Near-Resonant Two-Photon Excitation of CN

5. FUNDING NUMBERS

IL161102AH43

6. AUTHOR(S)

John A. Guthrie,* William R. Anderson, Anthony J. Kotlar, Yuhui Huang,** and Joshua B. Halpern**

7. PERFORMING ORGANIZATION NAME(S) AND ADDRESS(ES)

U.S. Army Research Laboratory
ATTN: AMSRL-WM-PC
Aberdeen Proving Ground, MD 21005-5066

8. PERFORMING ORGANIZATION REPORT NUMBER

ARL-TR-1382

9. SPONSORING/MONITORING AGENCY NAMES(S) AND ADDRESS(ES)

10.SPONSORING/MONITORING AGENCY REPORT NUMBER

11. SUPPLEMENTARY NOTES

*Present address: Department of Physics, University of Central Oklahoma, Edmond, OK 73034.
**Center for the Study of Terrestrial and Extraterrestrial Atmospheres, HowardUniversity, Washington, DC 20059.

12a. DISTRIBUTION/AVAILABILITY STATEMENT

Approved for public release; distribution is unlimited.

12b. DISTRIBUTION CODE

13. ABSTRACT ***(Maximum 200 words)***

Development of sensitive detection methods for CN is important because of applications to propellant flames. This radical plays a critical role in propellant combustion chemistry.

We have observed a strong two-photon absorption in the $B^2\Sigma^+$-$X^2\Sigma^+$ (3,0) band of CN by means of a resonant enhancement through the $A^2\Pi_i$, $v'=4$ level. Many lines are seen in the two-photon spectrum due to multiple single-photon near resonances in the $A^2\Pi_i$-$X^2\Sigma^+$ (4,0) band. The detuning of the laser from these resonances varies from less than one to hundreds of wavenumbers, producing unusually large peak-intensity variations in the two-photon spectrum. This effect is not observed in two-photon transitions far from resonance. Resonant enhancement is observed over a range from $N = 5$ to 20. We know of no other molecular two-photon transition in which a near resonance produces such dramatically varying intensities over a short range of rotational levels. A calculation of the line strengths for these transitions reproduces the major features of the spectrum.

14. SUBJECT TERMS

cyanide radical, combustion diagnostics, two-photon transition

15. NUMBER OF PAGES

26

16. PRICE CODE

17. SECURITY CLASSIFICATION OF REPORT	18. SECURITY CLASSIFICATION OF THIS PAGE	19. SECURITY CLASSIFICATION OF ABSTRACT	20. LIMITATION OF ABSTRACT
UNCLASSIFIED	UNCLASSIFIED	UNCLASSIFIED	

INTENTIONALLY LEFT BLANK.

USER EVALUATION SHEET/CHANGE OF ADDRESS

This Laboratory undertakes a continuing effort to improve the quality of the reports it publishes. Your comments/answers to the items/questions below will aid us in our efforts.

1. ARL Report Number/Author ARL-TR-1382 (Guthrie) Date of Report June 1997

2. Date Report Received _____

3. Does this report satisfy a need? (Comment on purpose, related project, or other area of interest for which the report will be used.) _____

4. Specifically, how is the report being used? (Information source, design data, procedure, source of ideas, etc.) _____

5. Has the information in this report led to any quantitative savings as far as man-hours or dollars saved, operating costs avoided, or efficiencies achieved, etc? If so, please elaborate. _____

6. General Comments. What do you think should be changed to improve future reports? (Indicate changes to organization, technical content, format, etc.) _____

CURRENT ADDRESS

_____
Organization

_____
Name E-mail Name

_____
Street or P.O. Box No.

_____
City, State, Zip Code

7. If indicating a Change of Address or Address Correction, please provide the Current or Correct address above and the Old or Incorrect address below.

OLD ADDRESS

_____
Organization

_____
Name

_____
Street or P.O. Box No.

_____
City, State, Zip Code

(Remove this sheet, fold as indicated, tape closed, and mail.)
(DO NOT STAPLE)

DEPARTMENT OF THE ARMY

OFFICIAL BUSINESS

NO POSTAGE
NECESSARY
IF MAILED
IN THE
UNITED STATES

BUSINESS REPLY MAIL
FIRST CLASS PERMIT NO 0001,APG,MD

POSTAGE WILL BE PAID BY ADDRESSEE

DIRECTOR
US ARMY RESEARCH LABORATORY
ATTN AMSRL WM PC
ABERDEEN PROVING GROUND MD 21005-5066